Test of the validity of the gradient expansion for slowly-varying extended systems and coefficients of the sixth order for the KE in 1d

Joseph B. Dizon
Department of Chemistry, University of California, Irvine, CA 92697

Lucas O. Wagner, John C. Snyder, and Kieron Burke*
Department of Physics and Astronomy, University of California, Irvine, CA 92697
(Dated: June 14, 2012)

The calculation of the non-interacting KE is an incredible challenge. One could use the gradient expansion (GE) to calculate the non-interacting kinetic energy (KE) by the knowledge of the density alone. The system of interest was the cosine potential, which has a periodic potential that can approximately model solids. The density of cosine potential was are obtained by summing single-particle eigenfunctions that satisfying boundary conditions. The density depends on the potential V_0, the length of the unit cell d, the number of electrons per unit η, and the number of unit cells N_c, which was manipulated to explore the behavior of the GE. An extrapolation technique was introduced to calculate the KE within the thermodynamic limit where $N_c \to \infty$. An error analysis for the performance of the GE was implement by plotting the logarithm of percent errors against the order of the GE. The addition of the GE terms systematically improve KE calculations, and the sixth order GE performs the best for small V_0 and large η and d since the density becomes more slowly-varing. The sixth order term performs the best for large η and d and small V_0. However, the GE orders, particularly, the sixth order, breaks down completely for large V_0.

CONTENTS

I. Introduction 1

II. The gradient expansion of the kinetic energy 2

III. The density of the cosine potential 3

IV. The KE of the cosine potential and tools for analyzing the KE 5

V. Performance of the GE for varying V_0 7

VI. Performance of the GE for varying η 8

VII. Discussion 8

VIII. Conclusion 9

IX. Acknowledgements 10

References 10

I. INTRODUCTION

Electronic structure calculations in chemistry and physics may solving the interacting Schrödinger equation for the energy of the system which includes the kinetic energy (KE). However, calculations of the interacting KE are too slow and difficult to carry out, making them impractical to perform. Instead, the non-interacting KE is considered because it can be calculated with reasonable accuracy.

Density-functional theory has become a popular "work horse" for solving the electronic structure of atoms, molecules, and solids. The calculation of the non-interacting system, unlike the interacting system, involves the introduction of the Kohn-Sham (KS) scheme that calculates the components of the energy including non-interacting KE is obtained by using KS equations [1]. For the KS scheme to work, the energy must depend on the electronic density and from the HK theorem, the components of the energy are expressed as a functional of the density [2]. A functional, as defined in many DFT textbooks, assigns a number to a function [3]. In other words, one can calculate the energy by simply knowing the density. The non-interacting KE is of important interest because this makes up the large portion of the energy that seemingly cannot be calculated from the electronic density alone (while the potential energy can be based solely on the density.)

Although the KS scheme has made many tremendous contributions for finding electronic structure properties or molecules, atoms, and solids, the KS scheme becomes too slow and computationally costly for large systems. Even though the KS scheme was developed in the 1960's, there were attempts to write explicit formulas for the non-interacting KE functional without going through the KS scheme with reasonable efficiency and minimal computational cost since the birth of DFT in the late 1920's. One of the first attempts to carry out KE calculations was done by Thomas and Fermi: they expressed the KE functional that is exact for the uniform electron gas of constant density and approximated for the slowly-

* Also at Department of Chemistry, University of California, Irvine, CA 92697

varying density, which later became famously known as the Thomas-Fermi model [4, 5]. However, the KE from the TF model suffers for rapidly-varying density, as the latter fails to capture the changes of the density.

Because of the difficulties of the TF KE for rapidly-varying densities, the gradient expansion (GE) has become a weapon of choice to correct the TF KE [6]. The GE is an asymptotic expansion that takes account of changes in the density by including derivative terms of the density. The GE, by construction, only includes even derivative orders for the density, the odd derivative orders canceling through translation invariance [6]. Various tests with the GE from previous works show that the GE corrects the non-interacting KE for second and fourth orders and diverges beyond the fourth order due to asymptotic behavior at higher orders. As the result, the GE fails to correct the KE at higher orders [6]. Despite of the shortcomings of the GE due to the divergence at higher orders, there is still interest in understanding the behavior of the GE for simple 1-dimensional (1d) systems which will serve as motivation to generate new KE functionals.

The GE from L. Samaj and J. K. Percus [7] was selected for this study because it is believed that this GE can be used to calculate the KE for large 1d systems slowly-varying densities. This GE is formed by using a series of recursion formulas to generate the KE functional by including correction terms for the TF KE. Presently, the GE is expanded to the 6th order by using a computer algebra system like *Mathematica*. In addition, the GE is expected to perform better for slowly-varying density.

Extended periodic systems are widely studied because these systems describe and approximate the behavior of solids [8, 9]. One can figure out properties of solids such as band structures, band energies, and and band gaps [9, 10]. Solids of interest are comprised of many repeating unit cells [6]. One can model the solid by introducing a periodic potential that describes the repeating cell [9]. By doing so, one can obtain eigenfunctions that have the same periodicity as a periodic potential and satisfy periodic boundary conditions, which is useful to generate electronic densities that describe the location of electrons in a periodic lattice. One of the common periodic systems that is investigated to study solids is the Kronig Penney, which obtains band energies by solving the Schrödinger equation to get eigenfunctions that satisfies boundary conditions [8]. The cosine model is investigated in this study because this resembles solid that contains a cosine potential and one can determine eigenfunctions that satisfy boundary conditions [11]. By knowing the density, one can determine the density that retains boundary conditions from the eigenfunctions. In addition, there are a very few number of studies that used the GE to study extended systems like the cosine potential. The motivation for this project is to assess the performance of the GE for slowly-varying densities from the cosine potential to calculate the KE.

The investigation of the GE divided into multiple steps: Sec. II describes how to obtain terms of the GE. Sec. III shows how to get densities of the cosine potential from eigenfunctions with the requirement of satisfying periodic boundary conditions. Sec. IV includes the formulation of calculating of the exact KE from eigenfunctions, the TF model, and the GE using an extrapolation approach for an infinitely large system, and an error analysis of plotting the logarithm of the percent error against the order of the GE. Analyses of the performance of the GE is divided into two main areas: Sec. V assess the behavior of TF model and the GE by changing the potential V_0 for varying the size of the unit cell d and taking a high V_0 to examine where the GE fails. Sec. VI investigates the behavior of the TF model and the orders of the GE for changing the length of the unit cell d to identify the regime where GE performs the best. These analyses aim to explore the effects of increasing the order of the GE whether the KE becomes more accurate than the TF model. In addition, these analyses serve as an assessment to determine if the coefficients of the gradient at the sixth order is correct. Atomic units are carried for all calculations presented in this paper and the KE will always be referred to as the non-interacting KE.

II. THE GRADIENT EXPANSION OF THE KINETIC ENERGY

The calculation of the non-interacting KE T_s is one of the earliest challenges, and perhaps, one of the central problems in DFT. First, the formalism for expressing T_s as a functional of the density involves on integrating over all space [7]

$$T_s[n] = \int dx\ t_s(x) \tag{1}$$

where $t_s(x)$ is the non-interacting KE density dependent on the electronic density $n(x)$. Historically, there were attempts to express the KE densitiy directly to calculate the KE without going through the use of KS equation. The KE densitiy from the TF model in its alternative form [7, 12] for non-interacting same-spin fermions is

$$t_s^{TF} = \frac{\pi^2}{6} n^3(x) \tag{2}$$

where the factor $\pi^2/6$ a correction factor for treating with large 1d systems, and the KE calculated from the TF model by inserting into (1) becomes [12]

$$T_s^{TF}[n] = \frac{\pi^2}{6} \int dx\ n^3(x). \tag{3}$$

The TF model does not always get an accurate KE since this is a local approximation without taking account changes of the density. The GE serves as an approach

to correct the TF KE by taking account gradient terms of the density. However, the GE is only used to treat slowly-varying densities and there is hope that truncting a certain number of correction terms can systematically improve the accuracy of the KE, which is an approach to treat asymptotic expansions.

Samaj and Percus generated their form of the GE by using a series of recursion formulas that obtains the KE density for various orders [7]. The recursion formulation requires a fair amount of numerical work to expand at the sixth order. The GE for the KE incorporating (1) and (3) is formally written as

$$T_s^{GE}[n] = T_s^{TF}[n] + \int dx \ \left(t_s^{(2)}(x) + t_s^{(4)}(x) + ...\right) \quad (4)$$

and the second, fourth, and sixth orders of the KE densities obtained from the recursion formulas are [7]

$$t_s^{(2)}(x) = -\frac{1}{24}\frac{n'(x)^2}{n(x)} - \frac{1}{2}n''(x) \quad (5)$$

$$t_s^{(4)}(x) = \frac{1}{30}\frac{n'(x)^4}{\pi^2 n(x)^5} - \frac{23}{360}\frac{n'(x)^2 n''(x)}{\pi^2 n(x)^4} + \frac{1}{90}\frac{n''(x)^2}{\pi^2 n(x)^3} + \frac{7}{360}\frac{n'(x)n'''(x)}{\pi^2 n(x)^3} - \frac{1}{360}\frac{n^{(4)}(x)}{\pi^2 n(x)^2}. \quad (6)$$

$$\begin{aligned} t_s^{(6)}(x) = &-\frac{25}{81}\frac{n'(x)^6}{\pi^4 n(x)^9} + \frac{3419}{4320}\frac{n'(x)^4 n''(x)}{\pi^4 n(x)^8} - \frac{569}{1260}\frac{n'(x)^2 n''(x)^2}{\pi^4 n(x)^7} + \frac{179}{5670}\frac{n''(x)^3}{\pi^4 n(x)^6} - \frac{467}{2016}\frac{n'(x)^3 n'''(x)}{\pi^4 n(x)^7} \\ &+\frac{4507}{30240}\frac{n'(x)n''(x)n'''(x)}{\pi^4 n(x)^6} - \frac{107}{15120}\frac{n'''(x)^2}{\pi^4 n(x)^5} + \frac{1391}{30240}\frac{n'(x)^2 n^{(4)}(x)}{\pi^4 n(x)^6} - \frac{67}{6048}\frac{n''(x)n^{(4)}(x)}{\pi^4 n(x)^5} \\ &-\frac{11}{1890}\frac{n'(x)n^{(5)}(x)}{\pi^4 n(x)^5} + \frac{11}{30240}\frac{n^{(6)}(x)}{\pi^4 n(x)^4} \end{aligned} \quad (7)$$

The recursion formula still obtains the TF portion of the kinetic energy and obtains the second, fourth, and sixth-order KE density corrections for the KE density and these KE densities are integrated over all space to obtain corrections to the KE. The orders of the GE are determined by the combinations of the derivatives of the density, *i.e.* the second-order term includes $n''(x)$ and $(n'(x))^2$, the fourth-order term includes $n'(x)^4$, $n''(x)^2$, $n'''(x)n'(x)$, and $n^{(4)}(x)$, and so forth. The sixth-order has the most terms, which relies on having many gradient terms for the density. In addition, the determination of the sixth order GE is still a great interest because it is difficult to tell if this is the correct GE, but there is a chance to expand the GE to the eight order to verify if the sixth order is consistent. The second and fourth orders were confirmed to be consistent [7].

The GE from (4) and the correction terms (5), (6), and (7) were used for calculating the KE for the cosine potential. The knowledge of the density is an essential requirement to obtain T_s.

III. THE DENSITY OF THE COSINE POTENTIAL

The cosine potential is used to model extended periodic systems [11]. The cosine potential is expressed as

$$V(x) = -V_0 sin^2\left(\frac{\pi x}{d}\right) \quad (8)$$

which has a cosine term when one can rewrite (8) using trigonometric identities. From (8), V_0 is the depth of the potential and d is the length of the unit cell. The length of the crystal is $L = N_c d$ where N_c is the number of unit cells. The presence of the periodic potential like this cosine potential serves as a pertubation for the free-electron model, where the potential is constant and for convenience, is zero [9–11]. Periodic systems are treated as infinite systems to describe a solid [6]. The number of unit cells shall become extremely large, perhaps $N_c \to \infty$. This is the thermodynamic limit for the periodic system.

The first step of getting the density of the cosine potential is to obtain eigenfunctions using a single-particle Schrödinger equation inserting (8) as the potential, which is

$$-\frac{1}{2}\psi_j''(x) - V_0 sin^2\left(\frac{\pi x}{d}\right)\psi_j(x) = \epsilon_j \psi_j(x). \quad (9)$$

From (9), ϵ_j is the energy eigenvalue, $\psi_j(x)$ is the eigenfunction, and j indicates an individual orbital. In order to solve (9), an expression for ϵ_j must be known. Because of the cosine term, one can rewrite the Schrödinger in the form of a Mathieu differential equation [11]

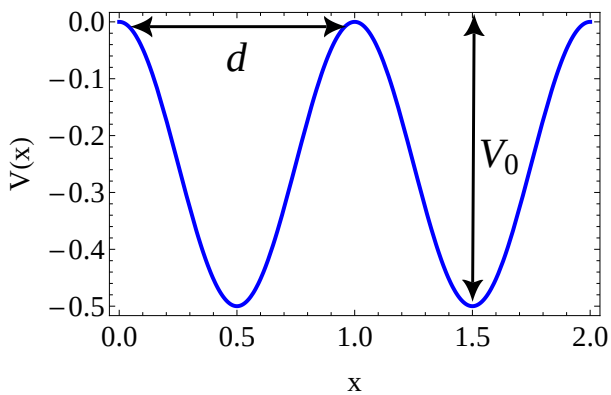

FIG. 1. Cosine potential with $d = 1$ and $N_c = 2$, and $V_0 = 0.5$.

$$y''(v) + (a - 2qcos(2v))y(v) = 0 \tag{10}$$

where a is the general characteristic value, q is the parameter, and v a variable to a function $y(v)$. By rearranging (9) in the form of (10), one can determine a, q, and ϵ_j, which are

$$a = \frac{d^2}{\pi^2}(V_0 + 2\epsilon), \tag{11}$$

$$q = \frac{V_0 d^2}{2\pi^2}, \tag{12}$$

and

$$\epsilon = \frac{1}{2}\left(\frac{\pi^2}{d^2}a - V_0\right). \tag{13}$$

Inserting (11), (12), and (13) into (9) obtains the general solution for the cosine potential. With the help of *Mathematica*, solving the Schrödinger equation gets an eigenfunction composed of Mathieu functions [11].

$$\psi_j(x) = A\,Ce\left(a, q, \frac{\pi x}{d}\right) + B\,Se\left(a, q, \frac{\pi x}{d}\right) \tag{14}$$

From (14), Ce is the even Mathieu function and Se is the odd Mathieu function. A and B are coefficients for the even and odd solution, respectively.

The periodic boundary conditions are necessary requirements to obtain periodic eigenfunctions. The eigenfunction must be continuous and differentiable at the entire length of the unit cell.

$$\psi_j(0) = \psi_j(L) \tag{15a}$$
$$\psi_j'(0) = \psi_j'(L) \tag{15b}$$

(15a) requires the eigenfunctions to be continuous and (15b) holds the condition of differentiability at the ends of the solid. (14) is broken into separate solutions that can satisfy conditions (15a) and (15b). To do so, one can select an eigenfunction depending on j. Writing the eigenfunction can be tricky since one needs to properly express the characteristic values for the even and odd Mathieu functions respectively. The characteristic values for the even Mathieu function is $a_{\frac{j}{N_c}}(q)$ and for the odd Mathieu function is $b_{\frac{j+1}{N_c}}(q)$. The advantage of expressing these characteristic values is the proper selection eigenfunctions based on the value of j. Both even and odd Mathieu functions behave as cosine and sine functions, respectively. Since normalization of sine and cosine functions are simple to carry, the normalization constants can be inserted into even and odd Mathieu functions, which are

$$\psi_{e,j}(x) = \sqrt{\frac{2}{L}}\,Ce\left(a_{\frac{j}{N_c}}(q), q, \frac{\pi x}{d}\right) \tag{16}$$

and

$$\psi_{o,j}(x) = \sqrt{\frac{2}{L}}\,Se\left(b_{\frac{j+1}{N_c}}(q), q, \frac{\pi x}{d}\right). \tag{17}$$

Once proper characteristic values for the even and odd Mathieu are obtained, one can select proper eigenfunctions by choosing integer values of j. The even solution from (17) is acceptable for $j = 0$ and even j. On the other hand, for odd j, (17) is appropriate. By following the pattern of selecting respectable eigenfunctions that meet conditions (15a) and (15b), The eigenfunction for the cosine potential selecting proper j values becomes

$$\psi_j(x) = \begin{cases} \psi_{e,j}(x) & j = 0, 2, 4, ... \\ \psi_{o,j}(x) & j = 1, 3, 5, ... \end{cases} \tag{18}$$

In addition, one can express the eigenvalues for each respective solutions from (16) and (17), which are essential for determining correct eigenfunctions.

$$\epsilon_j = \begin{cases} \frac{1}{2}\left(\frac{\pi^2}{d^2}a_{\frac{j}{N_c}}(q) - V_0\right) & j = 0, 2, 4, ... \\ \frac{1}{2}\left(\frac{\pi^2}{d^2}b_{\frac{j+1}{N_c}}(q) - V_0\right) & j = 1, 3, 5, ... \end{cases} \tag{19}$$

The eigenfunction from (18) are correct as long as this satisfies both sides of the Schrödinger equation while inserting the eigenvalue expression from (9). The eigenfunctions from (18) are real solutions for the cosine potential. One can plot appropriate eigenfunctions for each j.

From Fig. 2, the eigenfunction is even and has no nodes at $j = 0$. When $j = 1$, the eigenfunction is odd and has one node. When $j = 2$, the eigenfunction has two

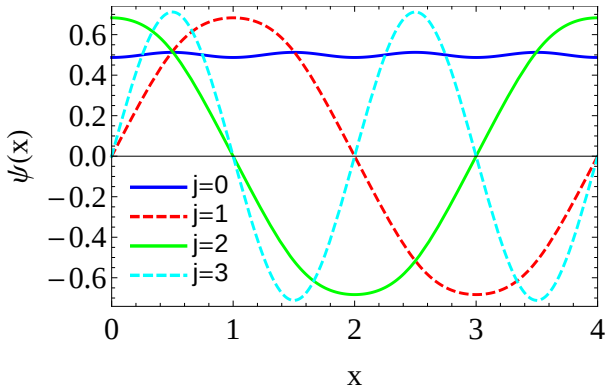

FIG. 2. Eigenfunctions for $j = 0$ (blue), 1 (red), 2 (green), and 3 (cyan) obtained from (18) and $d = 1$ and $N_c = 4$. Even eigenfunctions are solid and odd eigenfunctions are dashed lines.

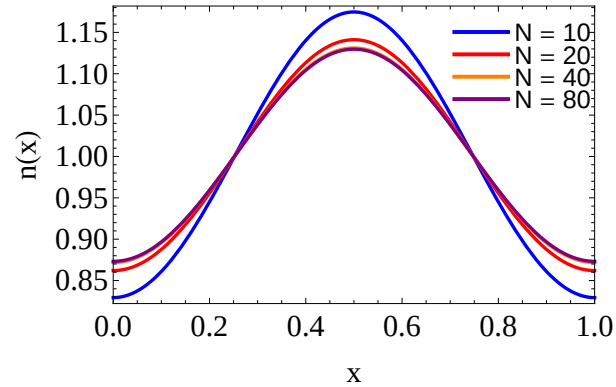

FIG. 3. Density for $\eta = 1$ with varying N_c and $V_0 = 1$.

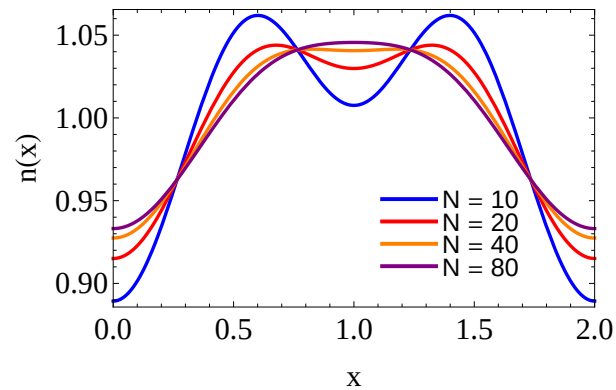

FIG. 4. Density for $\eta = 2$ with varying N_c and $V_0 = 1$.

nodes, and so forth. The values of j indicate the number of nodes for each eigenfunction and satisfying conditions (15a) and (15b).

The density of the cosine potential is composed of many single-particle eigenfunctions, which describes orbital that a single electron can occupy. One can express the density by summing the square moduli for each eigenfunction. In order to write the density, one munst know the number of electrons for the entire solid, which is N_e. Because the solid is comprised of many unit cells, one needs to know the number of electrons per unit η, which is determined from dividing the number of unit cells from N_e by the number of unit cells in the solid N_c. Therefore, the number of electrons is $N_e = \eta N_c$. Using this information, the density now becomes

$$n_\eta(x) = \sum_{j=0}^{\eta N_c - 1} |\psi_j(x)|^2 . \tag{20}$$

The construction of the density requires that $\eta = d$ to set the average density as $\bar{n} = \eta/d = 1$. This allows to add multiple number of electrons per unit cell in the solid for any given d. The nature of the density depends on d, η, and N_c. N_c is necessary to describe the size of the solid for a given η. By having a certain number of unit cells N_c, one can determine the converged limit of the density for large N_c with a given V_0.

There are different qualitative features for the following densites from Fig. 5 to 7. When $\eta = d = 1$, a single bump is present, two bumps are seen for $\eta = d = 2$, and for $\eta = d = 4$, four bumps are observed. The presence of these bumps indicate the number of electrons in a unit cell. Increasing η and d causes the densities to become more slowly-varying where fluctuations of the density become small. The beauty of the periodic system is that one can draw the density of a single unit cell without picturing the density of the entire system. In addition, the densities are continious and differentiable at the edges of the unit cell, which is a convenient feature for studying periodic systems. This also reveals that one can construct the density of the entire solid by simply using a single unit cell alone.

Aside from N_c, V_0 adjusts the shape of the density. The density becomes more slowly-varying for small V_0, and when $V_0 = 0$, the density becomes constant, which is a distinct feature of a uniform electron gas [3] and present in the free-electron model [8].

The challenge is to determine which condition of the density maximizes the performance of the GE, either by having small V_0 or large η.

IV. THE KE OF THE COSINE POTENTIAL AND TOOLS FOR ANALYZING THE KE

With the knowledge of the eigenfunction for the cosine potential from (18), one can calculate the KE [9].

$$t_j = \begin{cases} -\frac{1}{2d}\int_0^d dx\ \psi^*_{e,j}(x)\psi''_{e,j}(x) & j = 0, 2, 4, ... \\ -\frac{1}{2d}\int_0^d dx\ \psi^*_{o,j}(x)\psi''_{o,j}(x) & j = 1, 3, 5, ... \end{cases} \tag{21}$$

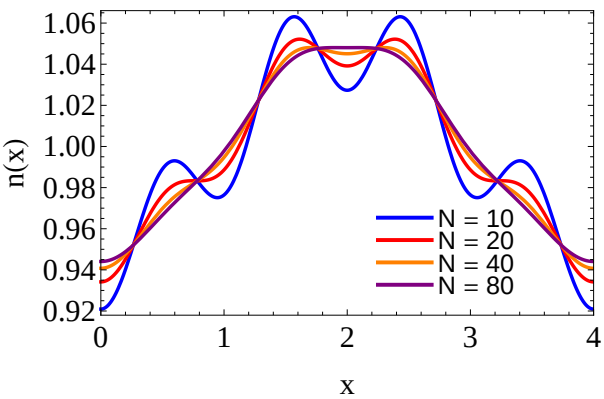

FIG. 5. Density for $\eta = 4$ with varying N_c and $V_0 = 1$.

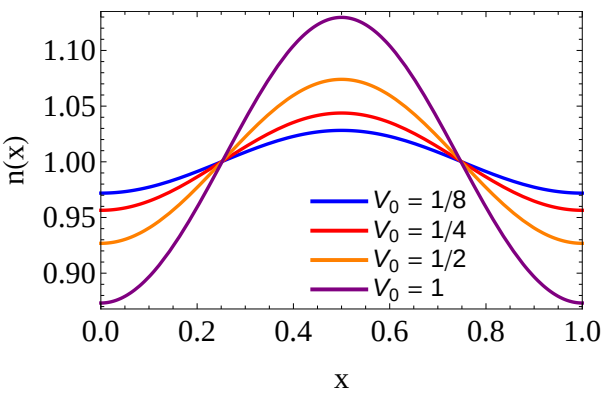

FIG. 6. Density for $\eta = 1$ and $N_c = 80$ for varying V_0.

(21) calculates the KE per unit length for a single unit cell rather than the KE for the entire solid. The procedure to sum the exact non-interacting KE for the entire solid is just like the approach from(20), which is

$$T_{s,\eta}^{EX} = \sum_{j=0}^{\eta N_c - 1} t_j. \tag{22}$$

The TF model and the GE calculates the KE by using (4) and dividing by d to get the KE per unit length, which the principle applies from (21). Due to the periodicity of the density for a unit cell, one can take advantage of calculating the KE without considering the entire solid. This procedure can minimize the cost of performing calculations for the KE for the remaining sections for this paper.

So far, calculations of the KE involve with a finite system, which has a finite number of unit cells N_c. The main goal is to calculate the KE at the thermodynamic limit, which is a key feature for a periodic system to describe a solid. One approach to carry calculations at the thermodynamic limit by using an extrapolation approach. In the extrapolation approach, one calculates the KE for the exact, TF, and the GE by choosing finite N_c values. After carrying calculations with different N_c, the KE is plotted against $1/N_c$. To determine the KE at the thermodynamic limit, one can obtain the y-intercept of the plot by taking constructing an approximate parabolic fit. By doing so, one can determine the KE by setting $1/N_c = 0$, which follows that $N_c \to \infty$. T_s as the KE for each N_c is evaluate for the exact, TF, and the GE. The KE is plotted against $1/Nc$ to generate an approximated quadratic plot. The KE at the thermodynamic limit is calculated by generating the fit and set $1/Nc = 0$, which is $N_c \to \infty$. The quadratic extrapolation for getting the KE at the thermodynamic limit is

$$f(z) = c_0\, z^2 + T_s^{\infty} \tag{23}$$

where c_0 is a coefficient determined from the quadratic fit, $z = 1/N_c$ is the variable for (23), and T_s^{∞} is the KE at the thermodynamic unit for the exact, TF, and the GE.

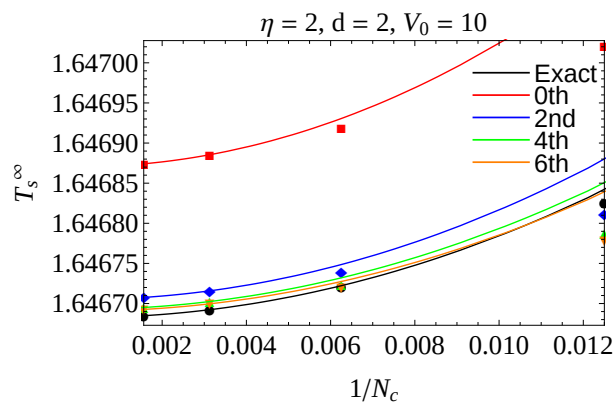

FIG. 7. Extrapolation plot for exact KE, TF, and the GE for $\eta = d = 2$ and $V_0 = 1/2$ using extrapolation points $N_c = 80, 60, 320$, and 640.

From Fig. 7, the extrapolation fits only perform well when $1/N_c$ is small. The difference between the TF and GE and the exact KE is evident as indicated by having different values of T_s^{∞}. To compare the performance of of the TF and the GE at the thermodynamic limit, one must compare these KEs with respect of the exact KE by computing the percent error

$$\%\Delta T_s^{\infty,p} = \frac{T_s^{\infty,p} - T_s^{\infty,EX}}{T_s^{\infty,EX}} \times 100\% \tag{24}$$

where $T_s^{\infty,p}$ is the KE for TF and the GE $T_s^{\infty,EX}$ is the exact KE, and p is the order of the GE expansion ($p = 0$ for TF, $p = 2, 4$, and 6 for the orders of the GE). For convenience, one can take logarithm of the percent error to describe order of magnitude of the error. A plot of the logarithm of the percent error against the order of the GE p serves as the benchmark to assess the performance of the GE.

V. PERFORMANCE OF THE GE FOR VARYING V_0

In this section, one can test the performance of the TF and the GE by adjusting V_0. A solid with unit cell length $d = 1$ and $\eta = 1$ and the solid with $d = \eta = 2$ are selected for this investigation. The plot of the logarithm of the percent error against the GE assess the performance of the GE here. Extrapolation points are used for $N_c = 10, 20, 40, 80$, and 160 to compute the KE at the thermodynamic limit.

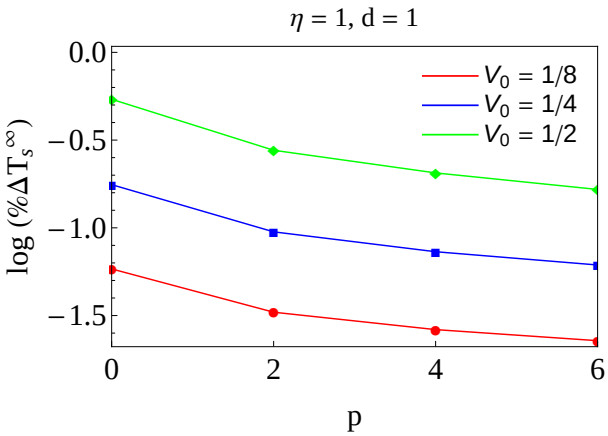

FIG. 8. Plotting the percent error of T_s^∞ vs. p for $\eta = d = 1$ for various V_0.

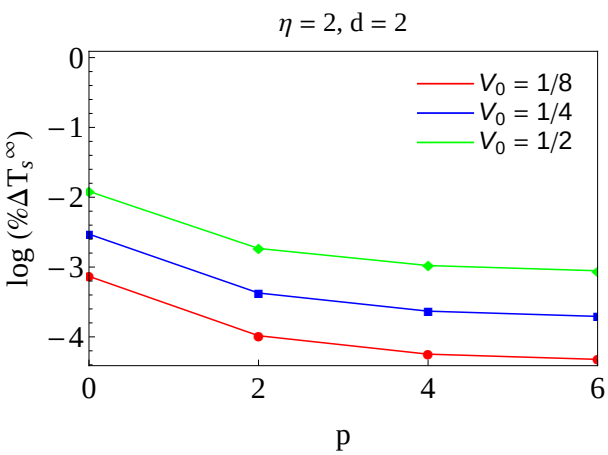

FIG. 9. Plotting the percent error of T_s^∞ vs. p for $\eta = d = 2$ for different V_0.

From Fig. 8, the errors for the KE calculations for different V_0 are not desirably accurate with an order of magnitude of 1 or 2. Each plot has a similar shape for different V_0 and this indicating the varying performance of the GE terms. The second order makes up the majority of the KE corrections and adding the fourth and sixth order improves the KE calculation although the contribution for the fourth and sixth order are not as much as the second order. From Fig. 9, the same behavior holds for the shape of the plots where the second order contributes larges to the KE correction while including the fourth and sixth orders slightly improve the accuracy of the KE. On the side note, the performance of the GE performs better for $\eta = d = 2$ and $\eta = d = 1$ where the error improves by order of magnitude btween 1 and 2. An in-depth focus for changing η and d is available on Sec. VI.

When V_0 becomes large, TF and the GE starts to fall apart for both $\eta = 1$ and $\eta = 2$.

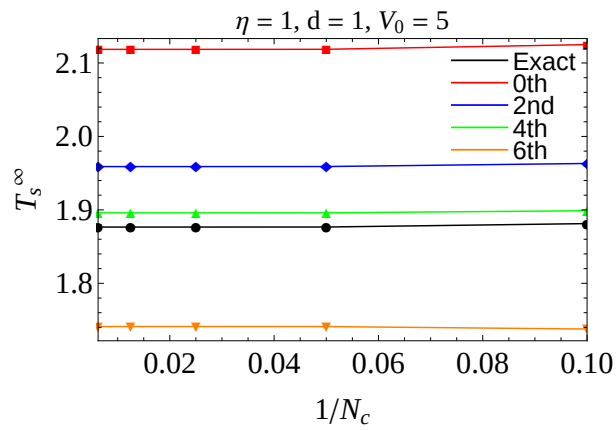

FIG. 10. Plotting T_s^∞ vs. $1/N_c$ for $\eta = d = 1$ for $V_0 = 5$.

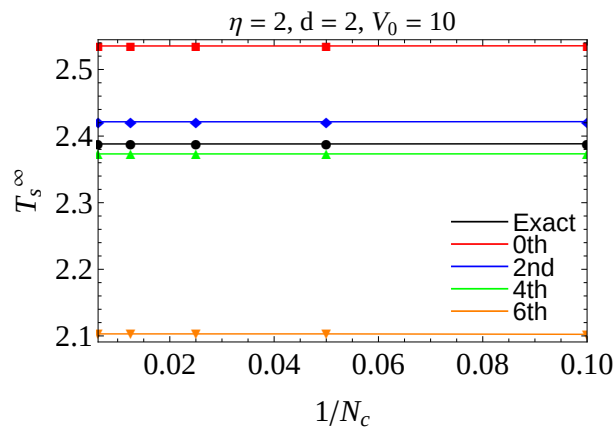

FIG. 11. Plotting T_s^∞ vs. $1/N_c$ for $\eta = d = 2$ for $V_0 = 10$.

The logarithm of the percent error is not applicable because GE underestimates the exact KE, which obtains a negative number. From Fig. 10 and 11, the plots of the TF and the GE do not line up with the exact KE, which reveals the breakdown of TF and the GE at large V_0 even at the thermodynamic limit. The sixth-order performs the worst, which severely underestimates the KE for both $\eta = 1$ and 2. On the other hand, the TF KE completely overestimates the KE for large V_0. Overall, the GE underperforms at large V_0

As a side note, the TF model and the GE are exact within the thermodynamic unit when $V_0 = 0$ because the density is constant.

VI. PERFORMANCE OF THE GE FOR VARYING η

This section explores the behavior of the GE with different η and d, holding an important condition that $\eta = d$ as described in Sec. IV. Large N_c values for the extrapolation approach are chosen to examine the behavior of the KE within the thermodynamic limit. In addition, calculations also include differerent values of V_0 to determine if the shapes of the $log(\%\Delta T_s)$ vs. p will have similar behavior and the shifts of the plots depend on V_0

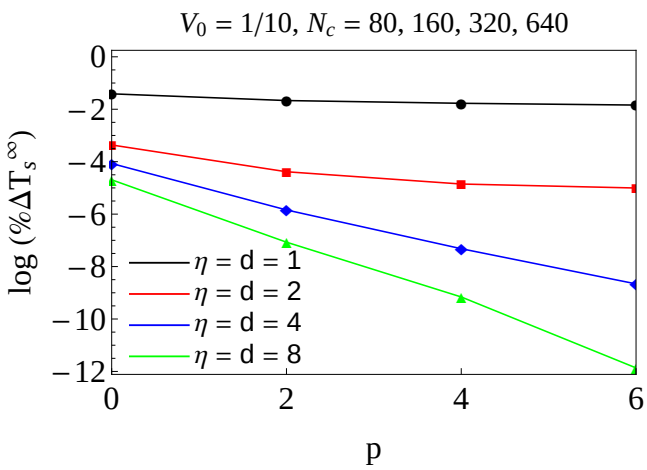

FIG. 12. Plotting the percent error of T_s^∞ vs. p for various η and d and $V_0 = 1/10$.

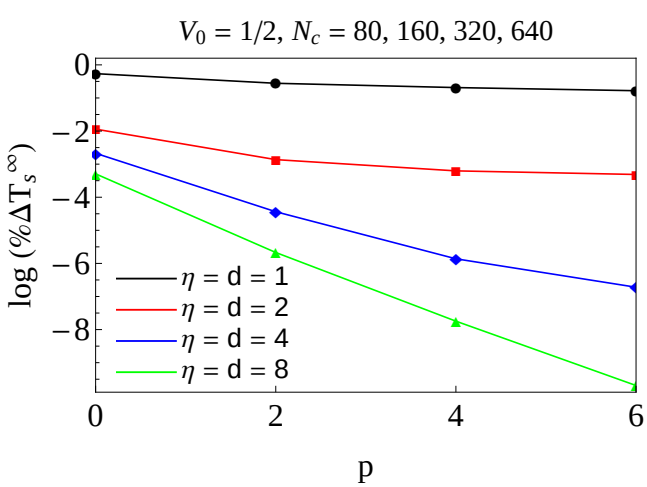

FIG. 13. Plotting the percent error of T_s^∞ vs. p for various η and d and $V_0 = 1/2$.

The extrapolation points are $N_c = 80, 160, 320$, and 640, which are used to obtain more accurate KEs at the thermodynamic limit than choosing smaller extrapolation points. In Fig. 12, the KEs for each η are more accurate for $V_0 = 1/10$ as indicated by a larger negative $log(\%\Delta T_s)$ than for $V_0 = 1/2$ from Fig. 13. The shapes are similar for each $\eta = 1$ and 2 with $p = 0, 2$, and 4, which the plots have a convex shape due to the slope between 0 and 2 is greater than the slope between 2 and 4. But including the sixth order GE reveal subtle different qualitative features for $\eta = 4$ and $\eta = 6$ with different V_0. For $V_0 = 1/2$ on Fig. 13, the plot for $\eta = 4$ is convex, where the slope of the line between $p = 4$ and 6 is smaller than the slopes at $p = 0$ and 2 and $p = 2$ and 4. For $\eta = 8$, the line is approximately linear. When $V_0 = 1/10$, the plot is linear for $\eta = 4$ and the plot is concave for $\eta = 8$ as indicated by a bigger slope between p values between 4 and 6 than p values between 0 and 2 and between 2 and 4.

Aside from different V_0 values, one can explore the general features from Fig. 12. For $\eta = 1$, the error improves by magnitude of 1 and 2, but performs least accurately among other solids. For $\eta = 2$, the error improves by magnitude of 3 and 4, which is a slight improvement over $\eta = 1$. The second order term makes up the majority of the KE correction indicated by the steepest slope as described earlier. For $\eta = 4$, the error to the KE improved to about the order of magnitude of 4 and 8, which is a better improvement over $\eta = 1$ and 2. The GE performs best at $\eta = 8$ since the order of magnitude of errors is extremely low, with the error improves by a magnitude of 4 for adding each GE order while the sixth-order contributes the most for correcting the TF KE.

VII. DISCUSSION

Calculations from Sec. V and Sec. VI present varying performances of the TF and the GE for different V_0, η, d, and extrapolation points for N_c. One can assess that the GE performs better for smaller V_0 as indicated by downward shifts of the $log(\%\Delta T_s)$ vs. p from Fig. 8, 9, 12, and 13. From these results, one can imply that decreasing V_0 makes the densities become more slowly-varying, causing the gradient of the density to become smaller. However from Fig. 8, the addition of terms of the GE at $\eta = 1$ improves the error slighly even for small V_0. One can say that the correction terms for higher orders of the GE become weaker even though adding those terms may improve the accuracy of obtaining the KE. In contrast, the errors for $\eta = 2$ improves by roughly an order of magnitude of 1 and 2 compared to $\eta = 1$ even though the shape of the curves is similar and higher order terms of the GE contributes less than at lower orders. Changing η has a significant effect on the performance of the TF and the GE, which shows that changing the length of the unit cell d and putting more electrons in the unit cell

can make the density become more slowly-varying than changing the potential with a small V_0. Moreover, this is evident from Fig. 12 and 13 that the errors of the GE becomes better for $\eta = 8$ than $\eta = 1, 2$, and 4, implying that the gradients of the density becomes weak. Therefore, the GE at the sixth order can significantly perform better than at lower orders.

The performance of each correction term of the GE varies with different η. Looking back at Fig. 8 and 9, the GE including the second-order term corrects the KE the most while including the fourth and sixth order slightly improves the KE, indicates that the dependence of the order is weak even though adding more terms makes the total KE calculation more accurate. The sixth order term only corrects the TF KE by a small fraction, which is smaller than including the second order term. But for high η, the addition of successive correction terms of the GE significantly improves the KE. Looking at $\eta = 4$ and $V_0 = 1/2$ from Fig. 13, adding orders of the GE improves the error by a magnitude of 2, which can tell that the dependence of the order is greater. Adding the sixth order term improves the TF KE, but does not improve the accuracy signifcantly. However, when $V_0 = 1/10$, the sixth order term significantly improves the TF KE by an order of magnitude of 4 in addition to big contributions from the second and fourth correction terms. This may show changing η has a tremendous effect on the overall performance of the GE. Perhaps one can assert that changing η has a substantial effect on changing behavior of the density, which influences the behavior of the GE.

When V_0 is large, the terms of the GE becomes erratic particularly at the sixth order. Before looking at the sixth order and from Fig. 10 and 11, TF badly overestimates the KE. The TF model is designed for the uniform electron glass and expects to behave poorly since changes in the density in terms of the gradients of the density are not included. The second order term for $\eta = 1$ and 2 significantly improves the KE but is still not close to the KE. Including the fourth order term improves the total KE, although this underestimates the exact KE for $\eta = 2$. The sixth order GE is the worst because this underestimates the exact KE completely where the sixth order term subtracts the total KE. This indicates that the sixth order term is sensitive to the gradients of the density, causing the KE to diverge way from the exact KE. The downfall of the sixth order GE comes from having strong gradients of the density where the density becomes rapidly-varying, causing the sixth order to behave unpredictably. The GE can only perform better for small V_0, particularly at the sixth order.

Looking back at Fig. 8, 9,12, and 13, one can safely say that the GE is asymptotic and systematically improves results as p grow for higher η and not much from smaller η, *i.e.* $\eta = 1$. One might come up with an appealing idea that expanding to the eight order can increase the accuracy of the KE based using the results to back up this claim. However, that notion is uncertain since no one has expanded the GE to the eight order. Computational cost using the recursion formulas from [7] become so immense that the eight order expansion becomes not feasable. If that is the case, one may not be sure to find out if the coefficients of the sixth order GE from (7) is correct since one must need to expand at higher order to check if the lower terms hold to be true, *i.e.* the sixth order expansion is consistent by expanding to the eight order and that is consistent if a tenth order expansion is accomplished. One may believe that increasing the order of the GE may further improve accuracy, but this idea can be true if the expansion to higher orders can be accomplished.

The extrapolation approach is only an approximation to get the KE at the thermodynamic limit because this approach selects finite values of N_c to generate a quadratic fit that obtains the y-intercept where $1/N_c = 0$ and $N_c \to \infty$. However, computational costs become severe for choosing high values of N_c to generate a quadratic fit since the number of terms of the density becomes high, causing the calculation KE by the GE to slow down significantly. However, the KE calculations for various $1/N_c$ do not always behave quadratically as indicated from Fig. 7, but the fits perform better when $1/N_c$ is extremely small. Perhaps, the extrapolation approach is a useful shortcut approach to determine the KE within the thermodynamic limit, which is useful to study periodic systems that model solids. Overall, the extrapolation approach can become more accurate for choosing higher N_c while sacrificing computational cost and time.

VIII. CONCLUSION

The calculations of the KE for the cosine potential reveal particular trends about the performance of the GE for various number of electrons per unit cell η, the unit cell length d, the potential V_0, and the number of unit cells N_c. The basis of these KE calculations involve on using the extrapolation approach to obtain the KE within the thermodynamic limit, which consequently, choosing high N_c values trades off between accuracy and more computational costs. The GE does fail for large V_0 since the density becomes rapidly-varying and the gradients of the density becomes bigger. The sixth order GE falls apart miserably where the sixth order term subtracts the total KE, which underestimates the exact KE. For small V_0 and large η, the addition of successive orders of the GE obtains the KE closer to the exact results. The sixth order GE performs the best because total KE is closer to the exact KE. However, the performance of the sixth order correction varies where the sixth order term corrects the KE by a slight fraction for smaller V_0 and small η. But for larger η, the sixth order terms corrects the total KE by larger fraction, improving the total KE. The improved performance of the GE for each successive order indicates that the GE can perform best when the gradient of the density is small when η is large and V_0 is small. Due to this trend, one may believe that expanding

towards the eight order can improve the accuracy of the KE, but this notion may or may not be true. If the eight order expansion is not carried, one may be uncertain if the sixth order expansion is correct. But despite of these short comings, the results and findings presented in this paper reveal fascinating trends and behaviors about the GE at least at the sixth order and the investigation of obtaining higher orders of the GE can be the subject for future investigation.

IX. ACKNOWLEDGEMENTS

I thank John Synder for his programming techniques on generating interactive plots and figures and codes for expanding the GE of the KE and helpful discussions about the GE. I thank Lucas Wagner for his contributions on understanding the formalisms of constructing eigenfunctions, densities, and the KE of the cosine potential, discussions and insights about the GE and the TF model, and his work for comparing his numerical results to the analytical results presented on this paper. I thank Prof. Burke for the opportunity to tackle the cosine potential problem and the GE project and his knowledgeable and insightful discussions and comments about the behavior of the GE, densities of the cosine potential, and procedures for analyzing results. I thank the Chem-SURP program for funding this project during the summer of 2011 and the Undergraduate Research Opportunities Program (UROP) for their support for undergraduate research. I am greatful to thank Prof. A.J. Shaka for his attentive support for the Honors Program in Chemistry in UC Irvine, undergraduate research and education, and his support for aspiring undegraduate researchers in the program.

[1] W. Kohn and L. J. Sham, "Self-consistent equations including exchange and correlation effects," Phys. Rev. **140**, A1133–A1138 (1965).

[2] P. Hohenberg and W. Kohn, "Inhomogeneous electron gas," Phys. Rev. **136**, B864–B871 (1964).

[3] E. Engel and R. M. Driezler, *Density Functional Theory: An Advanced Course* (Springer, New York, NY, 2011).

[4] L. H. Thomas, "The calculation of atomic fields," Math. Proc. Camb. Phil. Soc. **23**, 542–548 (1927).

[5] E. Fermi, "Eine statistische Methode zur Bestimmung einiger Eigenschaften des Atoms und ihre Anwendung auf die Theorie des periodischen Systems der Elemente (a statistical method for the determination of some atomic properties and the application of this method to the theory of the periodic system of elements)," Zeitschrift für Physik A Hadrons and Nuclei **48**, 73–79 (1928).

[6] F. Jansen, *Introduction to Computational Chemistry, 2nd Ed.* (Wiley, West Sussex , England, 2007).

[7] L. Samaj and J. K. Percus, "Recursion representation of gradient expansion for free fermion ground state in one dimension," The Journal of Chemical Physics **111**, 1809–1814 (1999).

[8] Estle T. L. Lane N. F. Morrison, M. A., *Quantum States of Atoms, Molecules, and Solids* (Prentice Hall, Englewood Cliffs, NJ, 1976).

[9] D. J. Griffiths, *Introduction to Quantum Mechanics, 2nd Ed.* (Pearson Prentice Hall, Upper Saddle River, NJ, 2005).

[10] R S. A. Ross J. Berry, R. S., *Physical Chemistry, 2nd Ed.* (Oxford University Press, New York, NY, 2000).

[11] T. R. Carver, "Mathieu's functions and electrons in a periodic lattice," Amer. J. Phys. **39**, 1225 (1971).

[12] K. Burke and L. Wagner, "DFT in a nutshell," (2011).